Dynamics of Cluster-Surface Collisions

Charles L. Cleveland and Uzi Landman

The structure, energetics, and dynamics of shock conditions generated in a nano-cluster upon impact on a crystalline surface are investigated with molecular-dynamics simulations for a 561-atom argon cluster incident with a velocity of 3 kilometers per second onto a sodium chloride surface. The "piling-up" shock phenomenon occurring upon impact, coupled with cascades of energy and momentum transfer processes and inertial confinement of material in the interior of the cluster, creates a transient medium lasting for about a picosecond and characterized by extreme local density, pressure, and kinetic temperature. The nano-shock conditions and impulsive nature of interactions in the newly formed compressed nonequilibrium environment open avenues for studying chemical reactivity and dynamics catalyzed via cluster impact.

Studies of impact phenomena have a long and interesting history (*1*, *2*), notably the investigations by Galileo (*3*) and Newton (*4*). Although early studies were concerned with the impact of rigid macroscopic bodies, later treatments allow for deformation processes (*5*). More recent work focused on impact processes involving finite aggregates (clusters) incident on target surfaces, with an emphasis on energy conversion to internal degrees of freedom (*2*) (vibrational, rotational, deformational, and electronic).

Collisions of particles with solid surfaces have been used extensively in modern investigations of surface structure and dynamics as well as in studies of the energetics, kinetics and dynamics of molecule-surface interactions, adsorption processes, reactions, and surface catalysis (*6*). Furthermore, techniques for surface processing and surface modification and methods of epitaxial film growth that make use of single-particle and particle-clusters impinging on surfaces have been proposed and implemented (*7*).

In this article we report the investigation of the dynamics of a collision between a finite medium-size atomic cluster and a solid surface. Motivating our study is the idea that energetic collisions of a many-body but finite, nanometer-scale, atomic or molecular aggregate (or "nano-cluster") with a surface (or between two such aggregates) could result in transient nonequilibrium conditions, akin to those occurring under shock conditions [as found in shock tubes, although as we show in the following the characteristic shock times in our case are orders of magnitude shorter than the microsecond times found in shock tube experiments (*8*)]. These extreme conditions and the impulsive nature (that is, dominated by momentum transfer) of interactions in the new cluster environment thus created may in turn initiate new modes of chemical reactions, occurring in a medium characterized by extreme density, pressure and kinetic-temperature conditions. Furthermore because of the extreme conditions that can develop in the cluster during the collision and the short transient characteristic times involved, the catalyzed reactions may well evolve in channels different from those governed by equilibrium kinetics. Considerations of reactions under shock conditions are not confined to laboratory shock-tube experiments, however. For example, it has been suggested (*9*) that synthesis of large molecules in interstellar clouds involves high-energy collisions between large clusters containing few thousand atoms, or between such clusters and solid grain surfaces. In addition, impact-shock synthesis of organic molecules on the early earth has been investigated (*10*). Moreover, shock waves have been invoked in studies of nuclear reactions, fusion, the nuclear equation of state, and heavy-ion collisions (*11*).

In an earlier study (*12*) we demonstrated that collisions between reactants embedded in clusters and incident reactants can be "catalyzed" by the cluster environment that serves as an extended third body (or local heat reservoir). Furthermore, we have suggested that this cluster-catalyzed reactivity (CCR), which may be nonelectronic in nature, may offer means for controlling the reaction pathways and branching ratios via variations in cluster size and the relative translational energy of the collision partners (*12*). Therefore, our study can be regarded as a continuation of our investigations of the avenues in chemical reactions and dynamics, and other physical processes, which cluster collisions may open (*12–14*). In this work we focus on consequences of the collision process pertaining to atomic (and ionic) motions, not including electronic excitations. Such excitations have been observed in recent experiments (*13*).

Most theoretical investigations of impact phenomena of projectiles on surfaces are of macroscopic nature (*15*). It has been recognized that proper treatment of collisions between clusters containing of the order of hundreds or thousands of molecules and solid surfaces requires considerations of atomic-scale energetics and dynamics to adequately account for energy deposition and redistribution as well as mass transport processes and to properly describe the spatial and temporal evolution of the system. Nevertheless, the number of investigations of cluster impact phenomena on the microscopic scale is rather small (*16*), and a full description of the dynamical evolution of such processes is lacking.

To explore the atomic-scale dynamics of the impact of a cluster on a surface it is natural to employ computer-based molecular dynamics simulations where the equations of motion of the interacting particles are integrated, and the analyses of the so obtained atomic phase-space trajectories yield information about the energetics, structure, and dynamics of the process with refined spatial and temporal resolution. Our molecular dynamics simulations of the collision of an initially vibrationally cold (T^0_{vib} = 50 K) Ar_{561} cluster impinging with a velocity of 3 km s^{-1} (a translational kinetic energy of 1.863 eV per particle) on a room temperature dynamic crystalline (001) surface of NaCl reveal major transfer of energy to the substrate and the formation of shock conditions in the cluster via a "piling-up" (or avalanche) process whereby the incident velocity of atoms in the front of the cluster is significantly reduced while the cluster atoms behind them continue their forward motion. The nano-shock phenomenon, expected to occur for other choices of collision partners, leads to severe compression of the cluster accompanied by extreme pressure (up to 10 to 12 GPa, where 1 GPa = 10^4 atm) and kinetic heating, propagating in a shock wave–like manner on a time scale of 1 to 2 ps. These conditions could induce and catalyze chemical and physical processes in a new, transient, nonequilibrium cluster environment, as well as activate surface modifications.

Molecular dynamics simulations. To investigate the atomic-scale mechanisms of energy conversion and redistribution and the dynamics of formation of shock conditions during the collision of a vibrationally cold Ar_{561} cluster with the (001) surface of a room temperature NaCl crystal, we have used molecular dynamics simulations. In this method the Newtonian equations of motion of a system of interacting particles

The authors are in the School of Physics, Georgia Institute of Technology, Atlanta, GA 30332.

are integrated by a computer, yielding phase-space trajectories (particles positions and momenta) and allowing exploration of the microscopic energetics, structure, and dynamics of the system.

In our molecular dynamics simulations the intracluster interactions between the argon atoms were described by pairwise 6-12 Lennard-Jones potentials (*17*) with a well depth $\epsilon = 0.01028$ eV and a length parameter $\sigma = 6.435\ a_0$ (where a_0 is the Bohr radius, 0.529 Å). The range of interaction was cut off at 20 a_0. The cluster system was equilibrated at 50 K outside the range of interaction with the substrate.

The calculational cell of the crystalline NaCl substrate (judiciously chosen to simulate a wide band gap material, thus minimizing substrate electronic excitations) consisted of six layers of dynamic particles with 784 particles per layer, arranged in the structure of a NaCl lattice and exposing the (001) surface. These layers were positioned on top of four layers of a static NaCl crystal of the same crystallographic orientation. The lattice parameter of the static substrate was chosen to be that of a NaCl bulk crystal at 300 K (10.66 a_0). The substrate calculational cell was repeated periodically in the two directions parallel to the (001) surface plane, with no boundary condition applied in the normal (z) direction (the cluster was not periodically repeated). The pairwise interactions between the ions of the NaCl substrate were described via potentials developed by Catlow *et al.* (*18*), which include Coulomb and Born-Mayer repulsion terms, and provide a good description of the solid.

The crystalline substrate was initially equilibrated at 300 K. During the subsequent simulations of the collision of the cluster with the surface the temperature of the surface was controlled via application of stochastic collision thermalization (*19*) at 300 K to the bottom dynamic layer of the surface region (that is, the one closest to the static part of the substrate and away from the top surface region) with a stochastic collision frequency of 7.75×10^{-3} fs^{-1}. The interactions between Ar atoms and the Na^+ and Cl^- ions of the substrate were described via the potentials developed by Ahlrichs *et al.* (*20*).

Subsequent to equilibration of the separated collision partners, a velocity of 3 km s^{-1} (that is, a kinetic energy of 1.863 eV per atom) was assigned to the cluster atoms (positioned outside the interaction range with the substrate) in the normal direction of incidence onto the substrate, and the equations of motion of the system were integrated using the fifth order Gear algorithm (*21*) with a time step $\Delta t = 0.25$ fs, which assures conservation of energy throughout the collision process. The numerically generated dynamical phase-space trajectories, and several other properties of the system, were recorded and subsequently analyzed. Among these properties we note the calculation of the pressure that was obtained from one-third of the trace of the atomic stress tensor, containing both a kinetic energy and virial contributions (*22*). In computing the atomic stress tensor the mass flow component of the velocity of a set of particles, here the velocity of their center of mass, was excluded (that is, only the "thermal" contributions are considered, see below).

Energetics of the system. A sequence of simulated atomic configurations was recorded at selected times during the interaction of the cluster with the surface (Fig. 1). The general characteristics of the evolution of the defor-

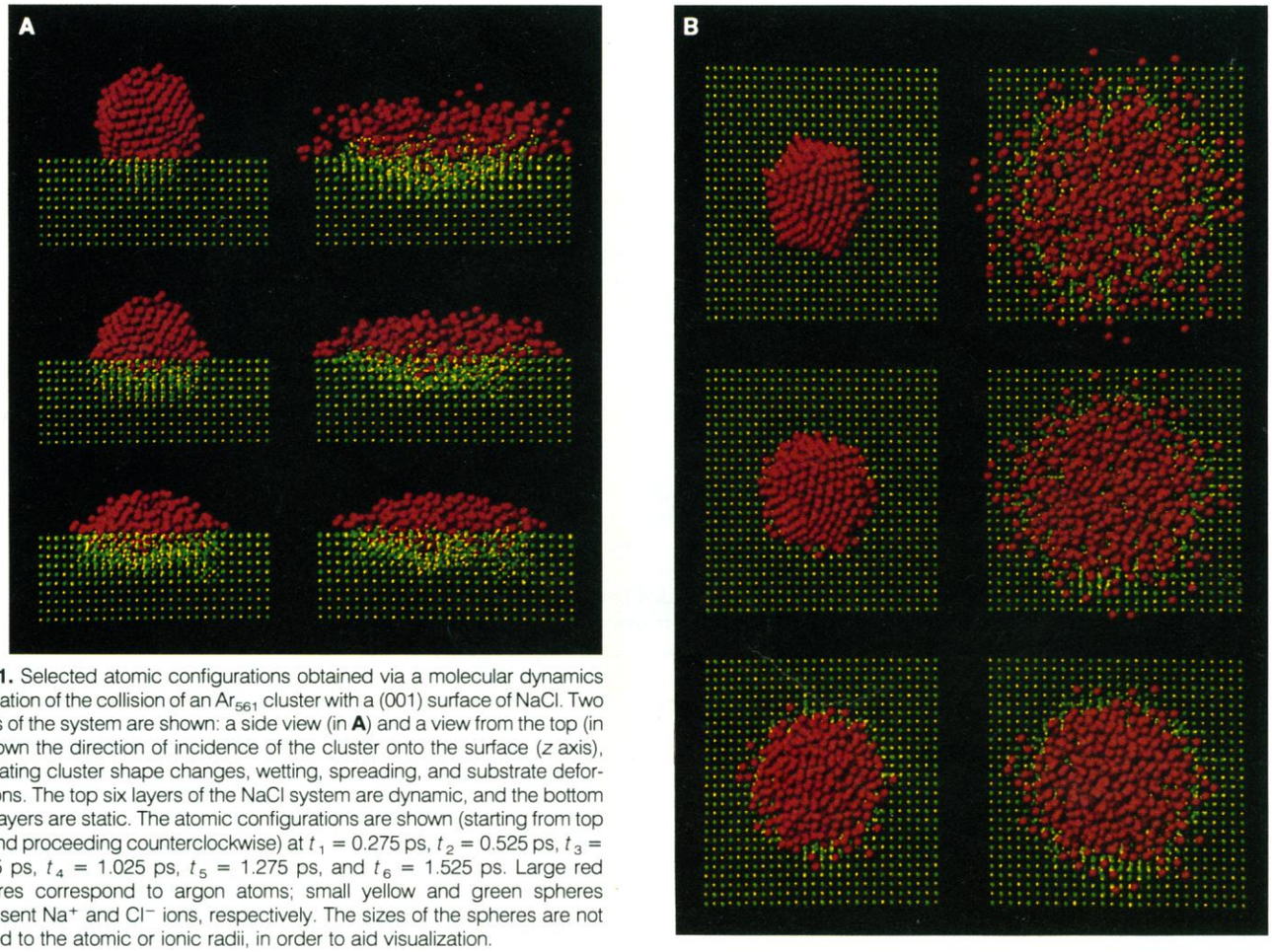

Fig. 1. Selected atomic configurations obtained via a molecular dynamics simulation of the collision of an Ar_{561} cluster with a (001) surface of NaCl. Two views of the system are shown: a side view (in **A**) and a view from the top (in **B**) down the direction of incidence of the cluster onto the surface (z axis), illustrating cluster shape changes, wetting, spreading, and substrate deformations. The top six layers of the NaCl system are dynamic, and the bottom four layers are static. The atomic configurations are shown (starting from top left and proceeding counterclockwise) at $t_1 = 0.275$ ps, $t_2 = 0.525$ ps, $t_3 = 0.775$ ps, $t_4 = 1.025$ ps, $t_5 = 1.275$ ps, and $t_6 = 1.525$ ps. Large red spheres correspond to argon atoms; small yellow and green spheres represent Na^+ and Cl^- ions, respectively. The sizes of the spheres are not scaled to the atomic or ionic radii, in order to aid visualization.

mation and shape of the cluster during the collision with the surface are reminiscent of those portrayed in photographs of a macroscopic liquid droplet colliding with a solid surface (*23*). However, owing to the relatively high incident velocity in our case, the impact of the cluster on the surface causes a large deformation of the substrate, localized about the impact area of the cluster with the surface. This deformation, extending several layers deep into the surface, involves penetration of cluster argon atoms into the substrate, collision cascades, local disruption of the lattice structure, and some mixing of the solid and cluster atoms. Additionally the strong perturbation at the surface region propagates into the solid as well as the cluster, resulting in spreading and partial evaporation. However, much of the cluster maintains its original shape up to $t \sim 0.5$ ps.

In discussing the energetics of the system it is instructive to distinguish a kinetic energy component representing overall flow in the system (K^f) from an internal kinetic energy (K^{int}) component corresponding to particles' "thermal" motion. This decomposition is particularly useful for the cluster. Therefore, when we refer to the total energy of the cluster or substrate atoms (E_c or E_s, respectively), the energy is the sum of potential and kinetic energy contributions with the latter calculated from the actual particle velocities obtained via the integration of the equations of motion. The internal kinetic energy we take to be the kinetic energy in a coordinate system co-moving with the cluster's center of mass, so that the "internal energy" (E_c^{int}) is just the sum of its potential energy and internal kinetic energy. In equilibrium steady-state conditions the equipartition of energy between the various degrees of freedom results in a direct relation between the internal temperature (or temperature for short) of a set of particles and the average of the internal kinetic energy ($3Nk_BT/2 = \langle K_N^{int} \rangle$, where k_B is the Boltzmann constant, and K_N^{int} is the internal kinetic energy of the N particles). Throughout most of the collision process we do not expect that equilibrium conditions will be achieved. Nevertheless, for comparative purposes we often express the kinetic energy of a set of particles as their kinetic temperature (both for internal and flow kinetic energies).

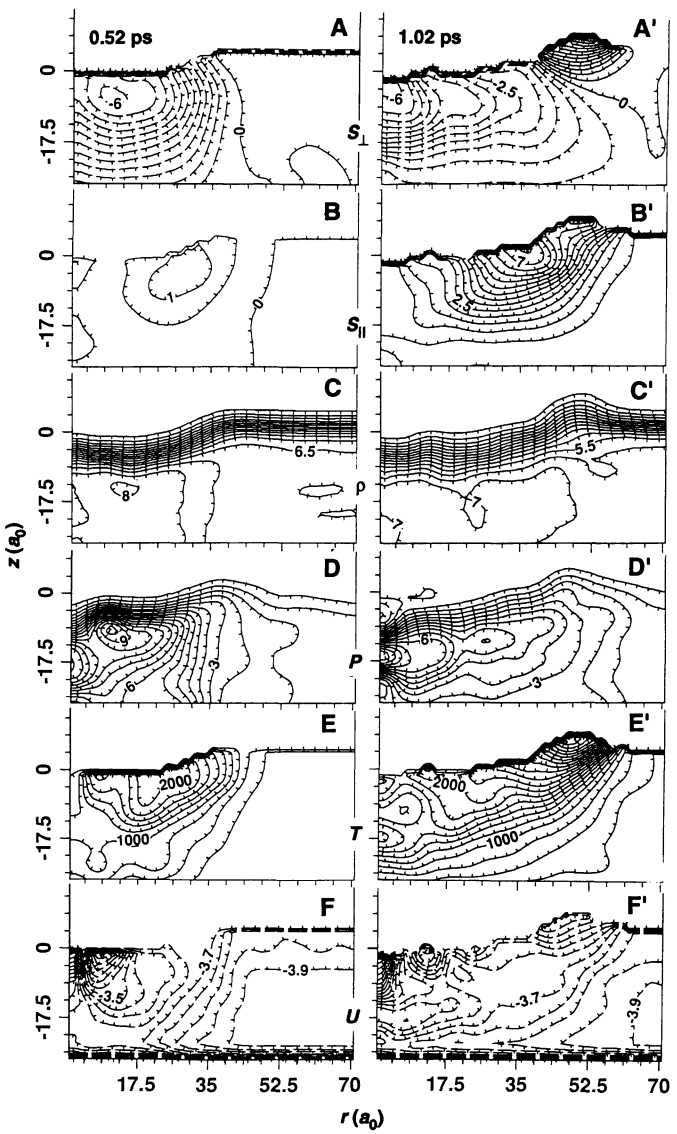

Fig. 2. Contours of properties of the dynamic NaCl (001) surface at t = 520 fs (left column) and t = 1020 fs (right column) during the collision of Ar_{561} with the substrate. In calculating the contours of a property at any given region the value of the property was weighed by a Gaussian of width 3 a_0 (*24*). Contours of atomic displacements from the initial positions (**A** and **A'**) in the z direction ($s_\perp$) and (**B** and **B'**) in directions parallel to the (001) surface ($s_\parallel$). Dashed contours correspond to $s_\perp$ downward displacements along the direction of incidence of the cluster. Note the increase in $s_\parallel$ (B') when compared to the earlier time (B), and the bulging of the substrate at the periphery of the impact area at the later time. The increment between neighboring contours Δ_s = 0.5 a_0. (**C** and **C'**) Density contours (in units of $10^{-3} \times a_0^{-3}$), with an increment $\Delta_\rho = 5 \times 10^{-4}\ a_0^{-3}$. The accumulation of contours near the surface is due to the transition from finite density of ions inside the substrate to vanishing values outside. (**D** and **D'**) Pressure contours (in units of gigapascals) with an increment Δ_P = 0.6 GPa. (**E** and **E'**) Kinetic-temperature contours (in units of degrees kelvin) with an increment Δ_T = 200K. (**F** and **F'**) Potential energy contours (per particle, in units of electron volts) with an increment $\Delta_U = 5 \times 10^{-2}$ eV. Distance is in units of a_0.

Substrate. We start with an analysis of the dynamics of the substrate during the collision. The impact of the cluster causes a significant deformation in the surface region of the substrate accompanied by some degree of implantation of argon atoms (Fig. 1). From Fig. 2, A and A', we observe that at early times the major downward displacement of substrate particles along the direction of incidence of the cluster are localized under the area of impact with a certain amount of bulging-up in regions surrounding this core region. The outside region is also seen to displace in the lateral direction (Figs. 2, B and B'). At the later time the core region is still displaced inwards (that is, the surface is indented) and the side-bulging develops further (see Fig. 2, A' and B', for $\tau \geq 35\ a_0$), as the deformation propagates in the substrate. These observations are also reflected in other quantities such as the density and pressure whose time and spatial variations are exhibited in Fig. 2, C and C' and D and D'; these figures also make evident the compression of the substrate caused by the cluster impact. As seen the transient compression results in densities up to 40 percent above the normal density of NaCl and the generation of a strong pressure pulse (up to ~10 GPa). The duration of these extreme density and pressure pulses is $\sim 0.5\ \text{ps} \lesssim \tau < 1$ ps.

Accompanying the compression is an increase in the energy of the perturbed substrate region. Although the potential energy behaves in a transient manner similar to that of the density and pressure, the temperature in the region increases rapidly to over six times room temperature, and the region remains thermally excited for a much longer time. Additionally, we observed that the kinetic temperature of particle motions in the z direction achieves a higher value than that associated with motions in directions parallel to the surface plane, and the relaxation of the latter is somewhat slower. The spatial propagation of the heat pulse in the substrate is evident from a comparison of Fig. 2, E and E'.

Finally, the contours of the surface potential energy at the two selected times

follow the spatial pattern of the displacement, density, and pressure (Fig. 2, F and F′). At both times the values of the potential energy at the central core region of the substrate (a cylindrically shaped region around the z axis of a radius and height of $\sim 15\ a_0$) are the highest in the substrate (less negative) because of the pronounced compaction of the region.

Cluster. To explore the local dynamical evolution during the collision process, we have monitored properties of the system at various regions of the cluster. These probe regions are defined as follows. Region $\mathcal{R}_0$ is a sphere with a radius $R = 9.2\ a_0$, centered at any time about the instantaneous center of mass of the cluster (initially this region contains the central atom and its 12 neighbors, and the initial number density in the region is $0.004\ a_0^{-3}$); regions $\mathcal{R}_-$ and $\mathcal{R}_+$ are defined in a similar manner with the center of regions $\mathcal{R}_-$ and $\mathcal{R}_+$ shifted with respect to the center-of-mass of the cluster along the axis normal to the surface (z) by $-R$ (region $\mathcal{R}_-$) and $+R$ (region $\mathcal{R}_+$).

The time variation of the flow kinetic energy in the various probe regions, expressed in units of temperature, T^f, shown in Fig. 3 (that is, the kinetic energy associated with the average velocity of the particles in a given region) illustrates the "piling-up" process. As seen, the translational flow kinetic energy, which at time $t = 0$ is equal to the incident energy corresponding to a velocity of 3 km s^{-1}, decreases sharply on impact. The onset time of the sharp decrease in T^f is offset from one region to the other, occurring earlier in the region closer to the front of the cluster (that is, closer to the solid surface). The decrease in T^f corresponds to conversion of the incident cluster translational energy to other energy components (potential and kinetic), and the offsets in the onsets of the sharp declines in T^f reflect the avalanche, or piling-up process, akin to shock formation and propagation. In order to further illustrate the sequential delayed nature of the process in the cluster in regions of increasing distance away from the solid surface we included in Fig. 3 the variation of T^f in an additional region in the cluster which is displaced with respect to the center-of-mass probe region ($\mathcal{R}_0$) by $+2R = 18.4\ a_0$.

The velocity of the piling-up process and the resulting shock in the cluster can be estimated from the differences in the times when the sharp declines in T^f begin to occur in the various probe regions (Fig. 3) and the known distances between the centers of these regions. From these data we estimate that the average velocity of shock-front propagation in the lower half of region $\mathcal{R}_0$ is ~ 6.5 km s^{-1}, decreasing to 3.9 km s^{-1} in the lower half of $\mathcal{R}_+$, and further decreasing to 2.8 km s^{-1} in the upper half of $\mathcal{R}_+$. Underlying the decrease in the front velocity in the direction away from the substrate surface is the fact that the lower part of the cluster is colliding with an ionic material that, while deforming, is stiffer than the cluster material (argon). Furthermore, the properties of the cluster influencing the velocity of propagation of disturbances in it (such as density, pressure, and internal kinetic temperature) are neither constant nor uniform during the collision, with the amplitude of these quantities decreasing as the disturbance reaches regions further away from the surface.

The overall energetics and the spatial and temporal evolution of the properties of the cluster during the collision are shown in Figs. 4 and 5. The energy in the cluster translational motion is converted partly to deformation, disruption of order, and vibrational excitation energy of the substrate (Fig. 4, E and F) and partly into potential and internal kinetic energy (heating) of the cluster atoms (Fig. 4, B and D). As seen from Fig. 4, A, B, and D, the decrease in the cluster translational energy is accompanied by an increase in the cluster potential energy, turning positive at $t \simeq 0.4$ ps and subsequently dropping sharply to a value below the initial potential energy of the cluster atoms, owing to the strong, attractive interaction between the argon atoms with the substrate ions. At the same time, the internal kinetic energy of the cluster increases markedly. These changes are caused by a compression of the system for $t \leq 0.75$ ps (as indicated by the density and pressure contours in Fig. 5) causing the

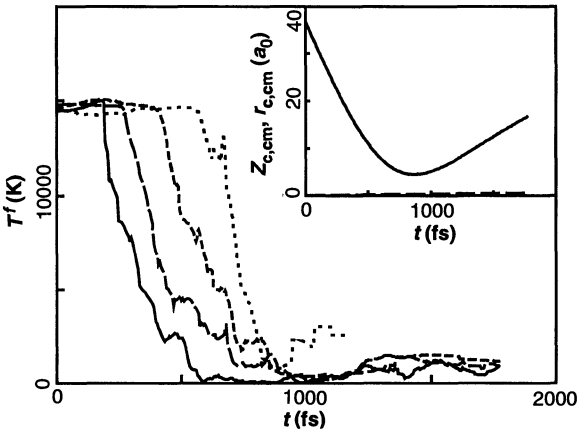

Fig. 3. Time histories of the flow kinetic energy expressed as temperature, T^f, in four probe-regions in the cluster; (solid line) region $\mathcal{R}_-$; (long dashed line) region $\mathcal{R}_0$; (short dashed line) region $\mathcal{R}_+$; and (dotted line) a region whose center is displaced upwards by 18.4 a_0 with respect to region $\mathcal{R}_0$. Note the time delay between the onset of slowing down which starts earlier in the region closest to the target surface (region $\mathcal{R}_-$). In the inset, we show the time variation of the location of the center-of-mass (cm) of the cluster (and thus the center of probe-region $\mathcal{R}_0$) during the collision. $z_{c,cm}$ (solid line) and $r_{c,cm}$ (dashed line) are the component of the center-of-mass location normal and parallel to the (001) surface, respectively. Note that the major variation is in $z_{c,cm}$. Temperature is in kelvins, time in femtoseconds, and distance in a_0.

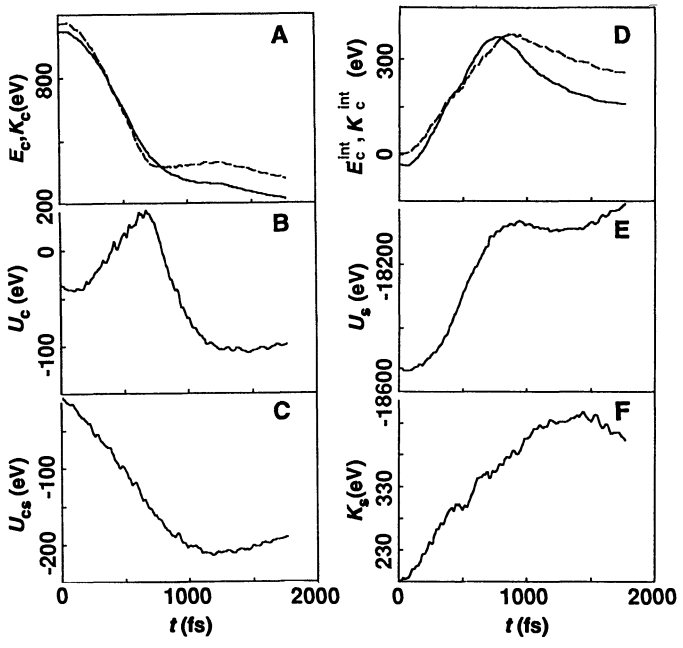

Fig. 4. Time variations during the collision of Ar_{561} with the (001) surface of NaCl in: (**A**) the total energy of the cluster (E_c, solid line) and of the total cluster kinetic energy (K_c, dashed line); (**B**) the potential energy of the cluster, U_c; (**C**) the interaction energy between the cluster atoms and the surface ions, U_{cs}; (**D**) the internal energy of the cluster (E_c^{int}, solid line) and the cluster internal kinetic energy (K_c^{int}, dashed line); and (**E** and **F**) substrate potential and kinetic energies, U_s and K_s, respectively. Energies are in units of electron volts, and time in femtoseconds.

atoms to experience repulsive interactions and less binding, and the subsequent decrease occurs on relaxation and spreading of the cluster. Indeed, the potential energy of interaction between the argon atoms and the substrate ions is attractive throughout (U_{cs}, in Fig. 4C). Associating half of U_{cs} with cluster atoms and half with substrate ions, and noting that the total potential energy of the cluster, U_c, contains contributions from both intracluster interactions and U_{cs}, we conclude (from Fig. 4, B and C) that the increase in the potential energy is associated with largely repulsive intracluster interactions, while the relaxation of the cluster, accompanied by spreading and increased binding to the surface ions, underlies the decrease of U_c, starting at $t \gtrsim 0.7$ ps (Fig. 4B). The relaxation of the potential energy, pressure, and density occurs at the faster rate than the internal kinetic energy of the cluster atoms. Throughout the simulation the substrate acts as if in contact with a thermal reservoir, via thermalization to 300 K at the bottom layer of the dynamic part of the substrate.

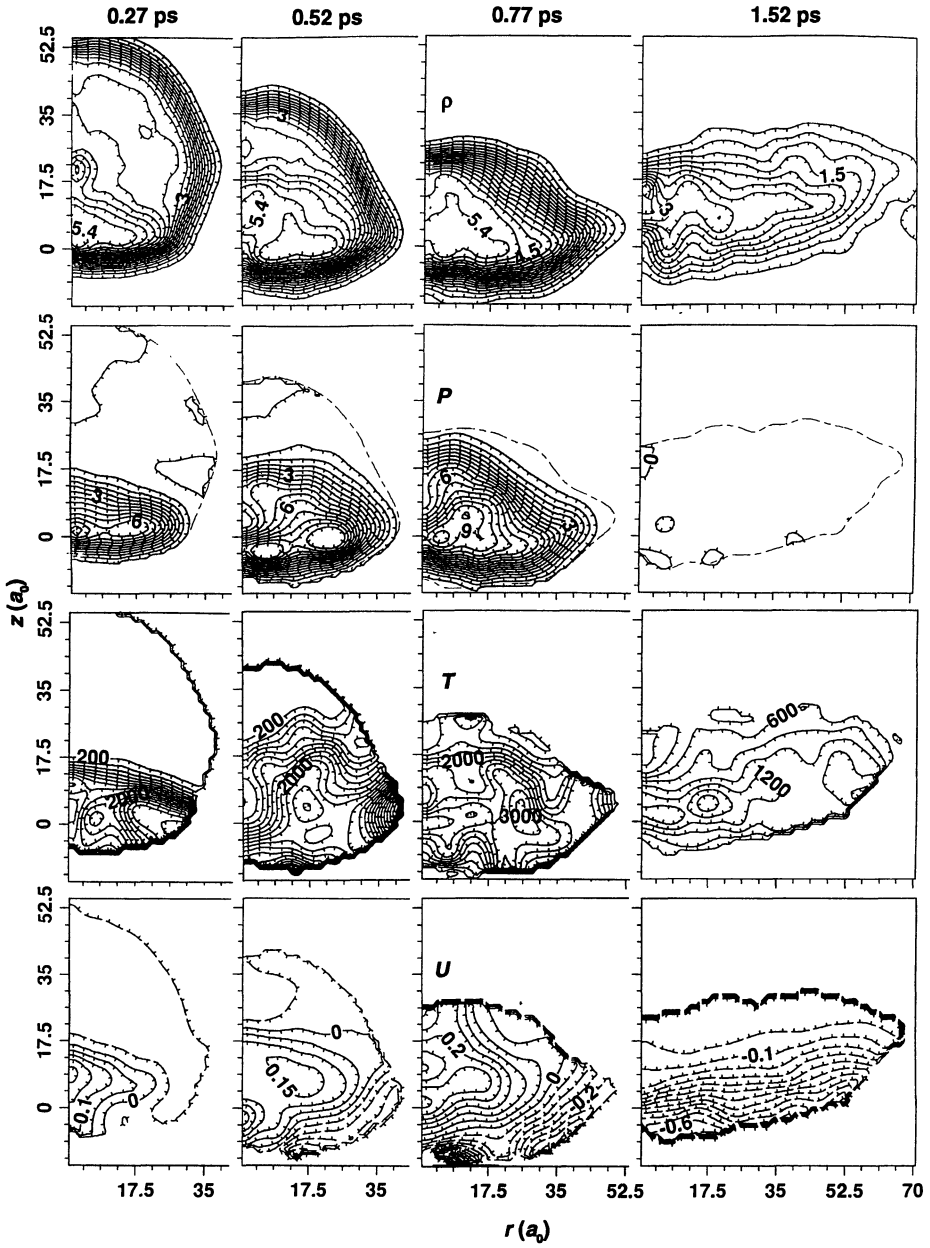

Fig. 5. Contours of density (ρ), pressure (P), internal kinetic temperature (T), and per particle potential energy (U_c) in the cluster (from top to bottom) at four selected times (across from left to right), t_1 = 0.27 ps, t_2 = 0.52 ps, t_3 = 0.77 ps, and t_4 = 1.52 ps during the collision with a solid surface [see (*24*) for a description of the construction of the contours]. In the pressure contour plots, we have added a dash-dotted curve which outlines the density-periphery of the cluster where ρ = 5 × 10^{-4} a_0^{-3}. Increments between neighboring contours are: Δ_ρ = 3 × 10^{-4} a_0^{-3}, Δ_P = 0.6 GPa, Δ_T = 200 K, and Δ_U = 5 × 10^{-2} eV. Values of selected contours are shown. Distances are in units of a_0.

From the contours shown in Fig. 5 (for t_1 = 0.27 ps, t_2 = 0.52 ps, t_3 = 0.77 ps, and t_4 = 1.52 ps, after the initial interaction between the cluster with the surface), we observe first that, as discussed before, the cluster penetrates the substrate region during the collision (see in particular the density contours at the top of Fig. 5). Moreover this process is accompanied by density and pressure pulses which emanate from the region of contact of the cluster with the surface (see ρ and P contours), propagating in a shock wave–like manner along the axis of the cluster in the direction opposite to the incident velocity as well as in approximately lateral directions corresponding to spreading and flattening of the cluster on the surface. However, the amplitudes of the density and pressure pulses are larger in the core region of the cluster near the z axis owing to inertial confinement of particles in the internal region of the cluster and the kinematics of the collision process. At later stages ($t > t_3$), the density in the cluster relaxes, dropping even below the original density (4 × 10^{-3} a_0^{-3}) and is more uniformly distributed throughout the flattened cluster (see ρ at t_4). This sequence of events is also portrayed by the pressure contours shown in Fig. 5, where for $t \simeq 1.5$ ps the pressure throughout the cluster dropped to below 1 GPa and is spread quite uniformly inside the cluster.

The internal kinetic temperature contours in the cluster exhibit also the propagation of a "heat" pulse emanating from the region of contact. However, we observe that the internal kinetic temperature rises at rather early stages (see T contours at t_2 and t_3) to high values (close to 3000 K) even in regions located radially further away from the axial internal region of the cluster (the cylindrical region about the z axis of radius ~15 to 25 a_0). This effect is mainly caused by relaxation of the cluster, starting in the peripherial regions of the cluster, in response to the compaction and pressurization of the cluster interior, coupled with the continued conversion of incident translational energy into thermal motion. These relaxation processes, which involve fast displacements of particles in the outside regions of the cluster, are reflected in the associated internal (thermal) kinetic temperature (T shown in Fig. 5).

Finally, from the potential energy contours (U) of the cluster atoms, we observe that at the initial stages of the collision ($t \lesssim t_2$) atoms at the bottom part of the cluster, in particular in the internal part of that region, acquire positive values, because of compression, while the shrinking region at the top of the cluster and the periphery of the cluster, especially the region of the cluster in contact with the surface, are characterized by negative values (the neg-

ative values at the cluster peripherial region are seen only in potential energy contours, since the increase in the kinetic energy in this region results in positive values for the total internal energy). Eventually, at about t_3 when the shock reaches the upper part of the cluster, most of the cluster is characterized by a positive potential energy except for small regions at the bottom and on the side of the cluster, where $U < 0$ owing to extra binding interaction energy between the substrate ions and the argon atoms and partial lateral relaxation, respectively. At a later stage (t_4), the relaxation covers the whole cluster (see negative potential energy contours for that time in Fig. 5). The effect is also exhibited in the total energy contours since at this stage both the compression and kinetic energy pulses have already traversed the lower part of the cluster resulting in negative values of the total energy.

It is of interest at this stage to contrast the above results, obtained via simulations where both the dynamics of the cluster and substrate atoms were included, with those where the substrate was treated as static. Comparison of results obtained via simulations for the two cases leads us to conclude that to achieve a faithful description of the collision process between a cluster and a solid surface (such as an ionic substrate) with incident velocities as high as used in this study (3 km s^{-1}) it is important to include the dynamical response of the substrate atoms in the simulation. Failure to do so results in a seriously inadequate description of the dynamics and energy conversion and distribution in the system, and consequently overestimation of the energy content in the cluster and excessively high values for the kinetic temperature and pressure during the collision.

Future prospects. We have studied with molecular dynamics simulations the collision of a medium-size atomic cluster containing 561 argon atom, equilibrated initially at 50 K, with a room temperature (001) surface of NaCl, with the cluster impinging on the substrate with a velocity of 3 km s^{-1} (energy of 1.863 eV per atom), investigating the atomic-scale energetics, structure, and dynamics of the process. Our findings demonstrate that the impact of the cluster on the surface results in a piling-up phenomenon leading to high-energy collision cascades and the development of a new transient medium in the cluster characterized by extreme density (up to 50 percent above normal liquid argon), pressure (in excess of 10 GPa), and temperature (kinetic heating of up to 4000 K) conditions, propagating in the cluster in a systematic shock wave–like manner, on a time scale of $\lesssim 1$ ps.

For the conditions of our simulations (impact velocity of 3 km s^{-1}) up to about three-fourths of the incident translational energy of the cluster is absorbed within 2 ps by the solid which undergoes severe deformation and disordering in a region localized about the impact area of the cluster and extending several layers into the substrate. Additionally we observe some degree of "implantation" of argon atoms in the disordered surface region of the surface. The compression in the substrate region results in densities of up to 40 percent above the normal density of NaCl and the generation of a strong pressure pulse (up to ~10 GPa). The duration of these extreme density and pressure pulses is 0.5 ps $\leq \tau <$ 1 ps. Subsequent relaxation of the surface is accompanied by bulging of the substrate in a region localized at the periphery of the cluster impact zone.

In simulations where the incident velocity of the cluster was taken to be 10 km s^{-1} (an order of magnitude larger incident energy), we observed massive damage to the surface and penetration of the cluster deep into the substrate. On the basis of these results we conclude that for the type of systems that we investigated the lower range of incidence velocities (1 to 3 km s^{-1}) is more appropriate in order to prevent excessive penetration of the cluster into the surface [note that even for the conditions of our study both the substrate and cluster undergo significant structural transformations (28)]. These consequences of the cluster-surface collision are expected to occur for other choices of the collision partners.

Our results suggest that in the presence of reactants embedded in the colliding cluster, or for clusters made of reactive constituents, such collisions could catalyze chemical reactions between cluster constituents as well as between cluster atoms or molecules and the surface material. Furthermore, because of the highly nonequilibrium nature of the new chemical medium generated via the collision, such reactions may well evolve in dynamic and kinetic pathways different from those governed by equilibrium thermodynamics considerations. In this study we focused on atomic dynamics excluding electronic excitations. Although such excitation effects will be included in future investigations of reactions, our results pertaining to the dynamics of the collision and the time development and characteristics of the new extreme cluster environment that evolves during the process are not expected to be modified in a substantial way by these effects.

Experimental realizations of collision systems such as the one investigated theoretically by us are possible. For example, several methods for generating charged clusters, which can be then accelerated to a desired impact velocity and impinge onto a solid surface, have been implemented and employed in the past several years, including the use of laser ablation (25), multiphoton ionization (26), and electron induced ionization (27). As possible choices of reactants and reactions we mention: O_2 and N_2 to yield NO, the dissociation of N_2O, the hydrogen-oxygen reaction, decomposition of ozone, the hydrogen-bromine reaction, H_2 and N_2 to yield ammonia, and pyrolysis and oxidation of hydrocarbons [this is just a short nonexhaustive list selected from shock-tube chemistry experiments (8)]. In addition "atomic thermometry" of the cluster during the collision process could be achieved via detection of light emission from atoms solvated (embedded) in the incident cluster and excited during the collision via impact with surrounding atoms. Such experiments would provide information about the degree of energy conversion and localization (in volumes of atomic or molecular dimensions) which while transient ($\lesssim 1$ ps) could be long enough (several vibrational periods) to allow for chemical processes to occur (barrier crossing, bond breaking, isomerization, and so forth).

REFERENCES AND NOTES

1. For a historical account see: T. Poeschl, *Der Stoss, Handbuch der Physic* (Springer, Berlin, 1926), vol. 6, chap. 7.
2. R. Beuhler and L. Friedman, *Chem. Rev.* **86**, 521 (1986).
3. G. Galileo, *Unterredungen und Demonstrationen Uber Zwei neue Wissenszweige' 1638 Ostwalds Klasser* (W. Engelmann, Leipzig, 1890–91), vol. 25, p. 38.
4. I. Newton, *Principia*, 1686, English translation by A. Motte (D. Adee, New York, 1848).
5. W. Goldsmith, *Impact* (Arnold, London, 1960).
6. T. Engel and K. H. Rieder, *Structural Studies of Surfaces with Atomic and Molecular Beam Diffraction* (Springer, Berlin, 1982); N. H. Tolk and J. C. Tully, Eds., *Inelastic Ion Surface Collisions* (Academic Press, New York, 1977); A. Zangwill, *Physics at Surfaces* (Cambridge Univ. Press, Cambridge, 1988); M. Van Hove and S. Y. Tong, Eds., *The Structure of Surfaces* (Springer, Berlin, 1985); R. Vanslow and R. Howe, Eds., *Chemistry and Physics of Solid Surfaces VII* (Springer, Berlin, 1988).
7. I. Yamada, G. H. Taksoka, H. Usui, T. Takagi, *J. Vac. Sci. Technol.* **A4**, 722 (1986); I. Yamada, *Appl. Surf. Sci.* **43**, 23 (1989); _____, G. H. Taksoka, H. Usui, S. K. Koh, *Mat. Res. Soc. Symp. Proc.* **206**, 383 (1991); T. Takugi, *Ionized-Cluster Beam Deposition and Epitaxy* (Noyes, Park Ridge, NJ, 1988); H. Haberland, M. Karrais, M. Mall, *Z. Phys. D* **20**, 413 (1991); J. Gspann, in *Proceedings of the 2nd International Conference on Clusters: From Clusters to Crystals*, P. Jenna, S. N. Khanna, B. K. Rao, Eds. (Kluwer, Boston, 1992); see (*2*); D. M. Manos and D. L. Flamm, Eds., *Plasma Etching: An Introduction* (Academic Press, New York, 1989); R. Kinslow, Ed., *High-Velocity Impact Phenomena* (Academic Press, New York, 1979); J. H. Weaver and G. D. Waddill, *Science* **251**, 1444 (1991); see articles in *Proceedings of the Second International Workshop on MeV and KeV Ion and Cluster Interactions with Surfaces and Materials* [*Colloq. Phys.*, Colloq. No. 2 (1989)].
8. J. N. Bradley, *Shock Waves in Chemistry and Physics* (Wiley, New York, 1962); Ya. B. Zeldovich and Yu. P. Raizer, *Physics of Shock Waves and High-Temperature Hydrodynamic Phenomena* (Academic Press, New York, 1967), vols. I and II.
9. W. W. Duly and D. A. Williams, *Interstellar Chem-*

istry (Academic Press, London, 1989).
10. C. Chyba and C. Sagan, *Nature* **355**, 125 (1992).
11. See articles in *Nuclear Equation of State, part A, Discovery of Nuclear Shock Waves and the EOS* (Plenum, New York, 1989); J. M. Eisenberg and W., Greiner, *Nuclear Models. Collective and Single-Particle Phenomena* (North-Holland, Amsterdam, ed. 3, 1987).
12. H.-P. Kaukonen, U. Landman and C. L. Cleveland, *J. Chem. Phys.* **95**, 4997 (1991).
13. For experiments of cluster-surface collisions see: U. Even, P. de Lange, H. Jonkman, J. Kommandeur, *Phys. Rev. Lett.* **56**, 965 (1986); R. J. Beuhler, G. Friedlander, L. Friedman, *ibid.* **63**, 1292 (1989); R. J. Beuhler, Y. Y. Chu, G. Friedlander, L. Friedman, W. Kinnman, *J. Phys. Chem.* **24**, 7665 (1990); R. D. Beck, P. St. John, M. L. Homer, R. L. Whetten, *Science* **253**, 879 (1991); *Chem. Phys. Lett.* **187**, 122 (1991); P. St. John, R. D. Beck, R. L. Whetten, in preparation.
14. For representative experiments of intercluster or molecule-cluster collisions see: J. L. Elkind, F. D. Weiss, J. M. Alford, R. T. Laaksonen, R. E. Smalley, *J. Chem. Phys.* **88**, 5215 (1988); W. D. Reents, Jr., and M. L. Mandich, *J. Phys. Chem.* **92**, 2908 (1988); W. F. Hoffman, E. K. Parks, S. J. Riley, *J. Chem. Phys.* **90**, 1526 (1989); Y. M. Hamrick and M. D. Morse, *J. Phys. Chem.* **93**, 6494 (1989); S. K. Loh, L. Lian, P. B. Armentrout, *J. Chem. Phys.* **91**, 6148 (1989); P. Fayet, A. Kaldor, D. M. Cox, *ibid.* **92**, 254 (1990); K. M. Creegan and M. F. Jarrold, *J. Am. Chem. Soc.* **112**, 3768 (1990); R. E. Leuchtner, A. C. Harms, A. W. Castleman, Jr., *J. Chem. Phys.* **92**, 6527 (1990); *ibid.* **91**, 2753 (1989).
15. See for example: Y. C. Huang, F. G. Hammitt, W.-J. Yang, *Trans. ASME* (June 1976), p. 276; P. E. O'Donoghue, S. R. Bodner, C. E. Anderson, Jr., M. Ravid, *Int. J. Impact Eng.* **8**, 289 (1989); F. H. Harlow and J. P. Shannon, *J. Appl. Phys.* **38**, 3855 (1967).
16. For some simulation studies, see: Y. Yamamura, I. Yamada, T. Takagi, *Nucl. Instrum. Methods Phys. Res. B* **37/38**, 902 (1989); Y. Yamamura, *ibid.* **45**, 707 (1990); M. H. Shapiro and T. A. Tombrello, *Phys. Rev. Lett.* **68**, 1613 (1992); K. H. Muller, *J. Appl. Phys.* **61**, 2516 (1987); H. Hsieh and R. S. Averback, *Phys. Rev. B* **42**, 5365 (1990); R. Biswas, G. S. Grest, C. M. Soukoulis, *ibid.* **36**, 6434 (1987); Xu Guo-Qin, R. J. Holland, S. L. Bernasek, J. C. Tully, *J. Chem. Phys.* **90**, 3831 (1989); *ibid.* **88**, 3376 (1988).
17. G. C. Maitland, M. Rigby, E. B. Smith, W. A. Wakeham, *Intermolecular Forces* (Clarendon Press, Oxford, 1981).
18. C. R. A. Catlow, K. M. Diller, M. J. Norgett, *J. Phys. C* **10**, 1395 (1977); in our calculations the effective second-neighbor $1/r^6$ term in the interionic interaction potentials was neglected.
19. J. R. Fox and H. C. Andersen, *J. Phys. Chem.* **88**, 4019 (1989).
20. R. Ahlrichs, H. J. Bohm, S. Brode, K. T. Tang, J. P. Toennies, *J. Chem. Phys.* **88**, 6290 (1988).
21. M. P. Allen and D. J. Tildesley, *Computer Simulations of Liquids* (Clarendon, Oxford, 1987).
22. T. Egami and D. Srolovitz, *J. Phys.* **12**, 2141 (1982).
23. S. Chandra and C. T. Avedisian, *Proc. R. Soc. London A* **432**, 13 (1991).
24. In calculating contours, the value of the exhibited property at any given spatial region was cylindrically averaged about the z axis and weighted by a Gaussian of width 3 a_0 in order to give a more continuous representation (that is, a certain degree of coarse-graining is applied to the discrete atomic system). Because of this Gaussian smoothing procedure an interfacial region (such as that between the surface of the cluster material and vacuum) appear somewhat diffuse. The high density of contours at such regions signifies the transition from finite values of the exhibited property inside the material to vanishing values outside it (see, for example, the substrate density contours shown in Fig. 2, C and C′). Dashed lines indicate contours corresponding to negative values of a property. To guide the eye, we have added one-sided tic marks on the contour lines, pointing in the direction of increase in values of the exhibited property.
25. J. B. Hopkins, J. B. Powers, R. S. Smalley, *J. Phys. Chem.* **85**, 3739 (1981).
26. D. Bahat, O. Cheshnovsky, U. Even, N. Lavie, Y. Magen, *ibid.* **91**, 2460 (1987).
27. T. P. Martin, *Phys. Rev.* **95**, 167 (1983); M. L. Alexander, M. A. Johnson, N. Levinger, W. C. Lineberger, *Phys. Rev. Lett.* **57**, 976 (1986).
28. For comparative molecular dynamics simulations of cluster impact with a velocity of 1 km s^{-1} (that is, a kinetic energy of 0.186 eV per atom), where shock formation with smaller amplitudes in ρ, P and T, and a much reduced surface damage have been observed, see H.-P. Cheng, C. L. Cleveland, U. Landman, in preparation.
29. Interesting conversations with U. Even and R. L. Whetten about cluster-surface collisions, at the formative stages of the research, are gratefully acknowledged. This work is supported by the U.S. Department of Energy, grant FG05-86ER45234. Calculations were performed at the Florida State Superconductor Center, through a computer-time grant from the DOE.

8 April 1992; accepted 11 June 1992